Palladium-manganese catalysts supported on monolith systems for methane combustion

J. Requies [a,*], M.C. Alvarez-Galvan [b], V.L. Barrio [a], P.L. Arias [a], J.F. Cambra [a],
M.B. Güemez [a], A. Manrique Carrera [c], V.A. de la Peña O'Shea [b], J.L.G. Fierro [b]

[a] Department of Chemical and Environmental Engineering, School of Engineering (UPV/EHU), 48013 Bilbao, Spain
[b] Institute of Catalysis and Petrochemistry, CSIC, Cantoblanco, 28049 Madrid, Spain
[c] KTH Deparment of Energy Technology/Heat and Power Tecnology, SE-10444 Stockholm, Sweden

Abstract

Alumina-supported bimetallic and monometallic Mn and Pd monolithic catalysts were prepared and tested in methane combustion. Two different reactor configurations were adopted for catalyst testing, i.e. a fixed-bed laboratory-scale reactor and a pilot-plant reactor which allowed work at different temperatures and pressures. The results of catalyst performance showed that all bimetallic catalysts are considerably more stable for methane combustion than the monometallic palladium catalyst. With the aim to explain the relationship between activity-stability and structure and surface properties, the catalysts were characterized by TPO, XRD, XPS and ICP-AES. The high stability displayed by the bimetallic systems is attributed to the influence of manganese in retarding the decomposition of PdO into metallic palladium. Thus, it appears that manganese oxides inhibit PdO decomposition, as a consequence of the increase in oxygen mobility in the manganese oxide spinel phase.
© 2007 Elsevier B.V. All rights reserved.

Keywords: Catalytic combustion; Methane; Palladium; Manganese; Monolith; Alumina

1. Introduction

Catalytic combustion is a promising technology for gas turbines, which has been shown to be an alternative to flame combustion for heat and power production [1,2]. Catalytic combustion is an environmental driven combustion technology to achieve ultra low emissions from gas turbines. Catalysts allow starting combustion well below the typical fuel lean flammability level, resulting in a lower adiabatic combustion temperature. This lower combustion temperature eliminates the large formation of thermal NOx and the combustion stability over the catalyst facilitates the fuel complete combustion. Besides, catalytic combustion also helps to reduce the emission of CO and other partially oxidized compounds.

In catalytic combustion, the reaction must start at the air compressor exit temperature (approximately 573–723 K) and must reach temperatures that assure total combustion [2]. This outlet temperature normally does not exceed 1573 K. Due to this different temperature range, there is no single catalyst material available able to work in the entire temperature range required for a catalytic combustor. For this reason, catalytic combustors are often divided into at least two segments, i.e. an ignition catalyst and a more thermally resistant catalyst. The ignition catalyst is located in the first segment of a catalytic combustor. Its task is to facilitate enough combustion reactions to raise the temperature of the compressor outlet gas to temperatures where the more thermally resistant catalysts igniters. If the ignition catalyst has not enough activity to ignite at the available temperature, pre-heaters are required. Pre-heaters cause an increase of fuel consumption, as well as elevated NOx emissions [3].

Therefore, different catalysts must be used. The ignition catalysts, usually with a precious metal as the catalytic phase, must be very active even at quiet low temperatures; medium temperature catalysts have to ignite at higher temperatures but still remain active despite combustion products generated in previous stages. Finally, high temperature catalysts must be active despite the highest temperatures generated and withstand

sintering, vaporization and ageing under severe conditions. Furthermore, all the catalysts employed must show high stability during operation. One of the great advantages of this system is that the catalysts will never be exposed to a temperature higher than 1223 K [4].

Pd/Al_2O_3 catalysts are commonly used for methane combustion [1–3,5]. They are very active at quiet low temperatures; therefore they are often used as igniters, but the catalysts based on palladium are also used for high temperature combustion [6,7]. The upper temperature limit of palladium use is about 1223–1273 K [8,9], below this range thermal sintering and vaporisation issues will be of less importance [4], palladium appear to show acceptable volatility at temperatures up to 1273 K [10]. However, palladium catalysts present one important drawback: they show high initial activity for methane combustion, but their activity is not stable. Thus, the PdO/Al_2O_3 catalyst deactivation is a major concern [11–15]. The addition of other metal oxides to alumina-supported palladium catalysts could be useful to enhance both catalytic activity and stability. Several authors have also examined the effects of different additives on the catalytic activity of PdO/Al_2O_3 catalysts [2,12,16]. These authors found that the addition of Pt into PdO/Al_2O_3 catalyst was effective not only in improving the catalytic activity, but also in preventing the catalyst deactivation in methane catalytic combustion. Other studies showed that the presence of Ag [17] or Rh [18] can improve the PdO/Al_2O_3 catalyst stability.

The aim of this study was to obtain similar results but with no-noble additives such as MnO_x. In a previous work [14], it was shown that Pd-Mn systems display better catalytic activity than the monometallic Pd catalysts and they have an ignition temperature of approximately 923 K (when the catalysts are calcinated at 1073 K). These characteristics indicate that these catalysts can be promising candidates for the high temperature stages. For this purpose Mn-Pd bimetallic catalysts of different compositions were prepared in order to investigate the catalytic combustion of methane under different operating conditions. Both the activity and stability of these catalysts have been evaluated. Characterization techniques such as TPO, XPS, XRD and ICP-AES have been used to investigate the structure, surface, red–ox properties and chemical compositions of mono and bimetallic manganese and palladium catalysts. These catalysts were prepared using a cordierite monolith substrate and gamma alumina as washcoat.

2. Experimental

2.1. Catalysts preparation

2.1.1. Preparation of monolithic catalysts

Different mono and bimetallic manganese and palladium monolithic catalysts were prepared for this study. Monolithic cordierite ceramic with 400 cpsi (Corning) was used to introduce a washcoat of alumina (18% with 3% La_2O_3, weight). Cylindrical blocks of ceramic monolith with size of 3 cm in diameter and 2 cm in length were obtained from large commercial ones.

The blocks were immersed in a solution of aqueous aluminum and lanthanum nitrate solutions (Al(NO_3)$_3$·9H_2O, Fluka, >98% and La(NO_3)$_3$·6H_2O 99.9%, Johnson Matthey as precursors) in a proper concentration to achieve a 9% washcoat. The impregnates were dried at 423 K for 2 h. This process was repeated until the solution was consumed. Then, the monoliths were calcined at 873 K for 4 h. This process was repeated to introduce the remaining 9% of washcoat, but now calcining at 1273 K for 2 h. After the introduction of alumina–lantana washcoat, manganese-containing monoliths were prepared by immersion in a solution of aqueous manganese nitrate solution (Mn(NO_3)$_2$·4H_2O, Panreac 98.5%, Johnson Matthey) as precursor in a proper concentration to achieve 18 wt% in the washcoat. Then they were dried at 423 K for 2 h. This process was repeated until the solution was consumed. Then, the monoliths were calcined at 773 K for 4 h.

Palladium-containing monoliths were prepared by wet immersion of alumina–lantana washcoated monoliths (with or without previous Mn incorporation) in solutions of aqueous palladium nitrate solution (palladium(II) nitrate dihydrate, Fluka, 40% Pd) as precursor, in proper concentrations to achieve 0.25, 0.5, 0.75 and 1 wt% in the washcoat. Then they were dried at 423 K for 2 h. This process was repeated until the solution was consumed. Then, the monoliths were calcined at 773 K for 4 h. Once prepared the six types of monolithic catalysts, they were subjected to a final thermal stabilization at 1273 K for 2 h. The nominal and real chemical composition of prepared catalysts is presented in Table 1.

2.1.2. Preparation of catalysts in powder

A commercial γ-alumina powder (Puralox HP-14/150, Condea) was used as a carrier to prepare manganese and palladium oxide catalysts. To decrease the loss of area during thermal treatment of alumina support 1 mol% La_2O_3 was added to alumina. The lanthanum promoter was introduced into non-stabilized alumina by wetness impregnation with an aqueous solution of lanthanum nitrate (La(NO_3)$_3$·6H_2O 99.9% Johnson Matthey). After impregnation, the lanthanum-containing support was dried at 423 K and calcined at 1273 K for 4 h. The Mn-containing catalyst, with a manganese loading of 18%, was prepared by impregnation with the appropriate amount of aqueous solution of manganese nitrate (Mn(NO_3)$_2$·4H_2O, Panreac, reagent grade) (4 ml of solution per gram of support) in a rotary evaporator at 353 K for 2 h. The precursors were then dried at 383 K for 4 h and then calcined in static air at 773 K for 4 h. Aliquots of this catalyst were subsequently used

Table 1
Labelling of catalysts and metal loading

Catalysts	Mn nominal (wt%)	Mn ICP-AES (wt%)	Pd nominal (wt%)	Pd ICP-AES (wt%)
5Mn	3.6	2	0	0
1Pd	0	0	0.20	0.10
5Mn-0.25Pd	3.6	1.3	0.05	0.04
5Mn-0.5Pd	3.6	2.7	0.10	0.08
5Mn-0.75Pd	3.6	3.5	0.15	0.12
5Mn-1Pd	3.6	2.5	0.20	0.14

to prepare the bimetallic Mn-Pd catalysts. For this purpose, proper amounts of palladium nitrate ($Pd(NO_3)_2 \cdot 2H_2O$) were employed to prepare two catalysts with 0.1 and 0.4 wt% palladium by wet impregnation. The procedure was the same as above for the raw monometallic Mn catalyst. The dried impregnates were calcined in air at 773 K for 4 h. This catalyst was then used to incorporate palladium. Thus, four binary palladium-manganese catalysts were prepared by consecutive impregnation of the manganese sample with aqueous solutions of the $Pd(NO_3) \cdot 2H_2O$ (Fluka, reagent grade). The volume of solution was selected to achieve a final composition of 0.25, 0.5, 0.75 and 1.0 wt% Pd. Drying and calcining was the same than in the manganese catalyst. For the sake of simplicity, these binary catalysts will be referred to hereafter as Mn-5 + Pdx (where 'x' stands for the palladium loading). An alumina-supported palladium catalyst, containing 1.0 wt% Pd, was also prepared according to the same procedure followed in the binary systems.

2.2. Catalysts characterization

2.2.1. ICP-AES

The manganese and palladium contents were determined by inductively coupled plasma atomic emission spectroscopy (ICP-AES), using a Perkin-Elmer Optima 3300DV apparatus, by dissolution of the ground samples in acid solutions.

2.2.2. TPO

The samples used for this analysis were not the result of catalyst monoliths grinding since the dilution originated by the cordierite would not allow to have enough sensitivity to determine the active phase red–ox profile. This analysis was performed using alumina-supported samples prepared as described in previous section. The red–ox properties of the catalysts were analyzed by temperature-programmed oxidation (TPO). These measurements were carried out using a Micromeritics TPD-TPR 2900 apparatus, equipped with a thermal conductivity detector. A continuous flow of 10% O_2/He was passed over 200 mg of calcined catalyst powder. The temperature was increased from room temperature to 1203 K at a rate of 10 K/min, followed by a decrease down to room temperature. The temperature cycle was repeated twice.

2.2.3. XRD

The phase compositions of the calcined samples (from monolith inside and outside walls) were analyzed by X-ray diffraction using a Panalytical X'Pert Pro Diffractometer operating with the following parameters: Cu Kα radiation, 45 mA, 40 kV, Ni filter, 2θ scanning range 5–80° and scan step size of 0.03. Phase identification was made using the reference database, supplied with the equipment.

2.2.4. XPS

The photoelectron spectra (XPS) were acquired with a VG Escalab 200R spectrometer equipped with a hemispherical electron analyser and an Al K$\alpha 1$ ($h\nu$ = 1486.6 eV, 1 eV = 1.6302×10^{-19} J) 120 W X-ray source. The samples,

in the form of a monolith layer, were mounted on a stainless steel sample holder, placed in the pre-treatment chamber and degassed at 573 K. The spectra were collected at pass energy of 20 eV, which is typical of high resolution conditions. Intensities were estimated by calculating the integral of each peak, after smoothing, subtraction of the S-shaped background, and fitting the experimental curve to Lorentzian and Gaussian lines (20% L/80% G). All binding energies (BE) were referred to Al 2p line at 74.5 eV.

2.3. Activity tests

The activity tests were performed in a lab-scale reactor and also in a pilot-scale plant. The tests were performed at different lambdas (λ = air/methane ratio) and temperatures. In the pilot-scale plant the reaction conditions were 5 bar and 823 K as inlet temperature. This pilot-scale plant is an adiabatic system with a maximum inlet temperature of 843 K. The combustion section is well insulated in order to achieve quasi-adiabatic operation (heat losses below 0.5%). Due to the limited inlet temperature (843 K) for catalytic activity tests at higher temperatures a lab-scale reactor facility was used. In order to end with comparable results, total pressure and lambda were the same in both systems.

2.3.1. Lab-scale reactor

The activity tests were carried out in a fixed-bed stainless steel tubular reactor (10 mm i.d. and 30 cm length), working at different pressures (from 5 to 12 bar). The monolith was placed in the middle of the reactor tube, and it was electrically heated in a furnace in order to maintain the desired temperature. The reaction mixture included CH_4, O_2 and inert (N_2) gases whose flows were adjusted by electronic controllers (Bronkhorst HiTech). The CH_4:O_2:N_2 molar ratio was different as a function of lambda, but the same linear velocity (around 0.9 m/s) was used in all of the experiments in the lab-scale reactor. The total flow was between 5611 mL/min (at 12 bar of pressure) and 2858 mL/min (at 5 bar of pressure) over the same monolith. These conditions correspond, respectively, to a WHSV of $2.87 \cdot 10^6$ and of $1.46 \cdot 10^6$ cm^3 g cat.$^{-1}$ h^{-1}, respectively. An initial temperature of 823 K was selected and then increased stepwise (50 K), until complete combustion was reached. Once a given temperature was reached it was maintained during 8 h, analyzing the reactor exit stream every 30 min. Analyses were carried out by an on-line GC equipped with FID and TCD detectors. Afterwards, stability tests were performed maintaining the reaction temperature at 1023 K for 100 h.

2.3.2. Pilot-scale plant

A pilot-scale plant was used in order to test the catalysts at operating conditions similar to the ones existing in to real gas turbine burners [19]: high pressure and high flow velocities (between 10 and 15 m/s). The test facility used consisted on a catalytic combustor, a fuel injection facility, a mixing system and electrical heaters which are located inside a cylindrical pressure vessel of 300 mm of diameter and 3 m of height. The size of the catalytic combustor is 35 mm of diameter and

Table 2
Analysis system and principle of the emission analysis

Emission component	Measuring instrument
NO, NO_2 and NO_x	Eco Physics CLD 700; EI Analyser (Chemiluminiscent)
CO	Fisher-Rosemount NGA 2000 (NDIR)
CO_2	Fisher-Rosemount NGA 2000 (NDIR)
O_2	Fisher-Rosemount NGA 2000 (Paramagnetic)
HC	J.U.M. Engineering FID 3-300A analyzer (FID)

500 mm of height. The test facility was supplied with compressed air from an external air supply system (by compressor piston type, 40 bar and 100 g/s). The air is heated with a group of electrical heaters. The maximum inlet temperature in this system is 873 K. The fuel (flow capacity of 2.5 kg/h) is methane with a purity of 99.999%. The fuel and air flows are controlled by mass-flow controllers. This pilot plant is fully equipped with instrumentation in order to collect information about flow rates, pressure, temperatures and gaseous emissions through on-line measuring instruments that are connected through 140 channels to a personal computer were all the data gathered are processed and stored. The emission measurements the corresponding analytical systems are indicated in Table 2.

The experiments were designed using an igniter and behind it the manganese-palladium catalyst bed. As the igniter a 5% Pd/γ-Al$_2$O$_3$ catalyst was used and after this igniter two catalysts, 1% Pd//γ-Al$_2$O$_3$ or 5Mn-0.5Pd/γ-Al$_2$O$_3$, were tested.

3. Results

Both the actual and the nominal compositions of the prepared catalysts are presented in Table 1. The actual catalyst compositions in the alumina washcoat are lower than the

nominal ones. The monolith preparation implied further active phase dilution.

3.1. X-ray diffraction

X-ray diffraction analysis was performed on the surface of the monolith inside and outside wall after calcination in air (1273 K). The diffraction peaks (Figs. 1 and 2) corresponding to the different active phases are masked by the cordierite diffraction lines. Unfortunately, the presence of the cordierite does not allow the estimation of the mean crystallite size of palladium or palladium oxide with this technique. Nevertheless, XRD analysis provides valuable information about the nature of different phases present in these catalysts.

The results of XRD are summarized in Table 3 and the interval for most intense diffraction peaks of palladium and manganese are presented in Fig. 2. In the 5Mn catalyst diffractogram the presence of Mn_2O_3 inside the monolith and the presence of the Mn_3O_4 outside have been found, and also the presence of different species that constitute the cordierite and others, such as $MnAl_2O_4$, formed by the interaction between manganese and alumina during the calcination at very high temperature (1273 K) can also be observed. XRD patterns of the 5Mn-0.25Pd, 5Mn-0.75Pd and 5Mn-1Pd catalysts were essentially the same than that of the 5Mn sample, showing an increasing presence of the $MnAl_2O_4$ outside the monolith. For the catalyst 5Mn-0.5Pd, the absence of diffraction lines of manganese oxides or compounds formed by the interaction of manganese with alumina can be observed. Manganese oxides were not detected in the outside monolith wall in the catalysts with the smallest Pd contents (5Mn-0.25Pd and 5Mn-0.5Pd). This fact could be attributed in part to a highly dispersed manganese oxide phase. Therefore, as the lower detection limit of the X-ray technique is around 4 nm, it is inferred that crystal sizes of manganese phases are below that value for these
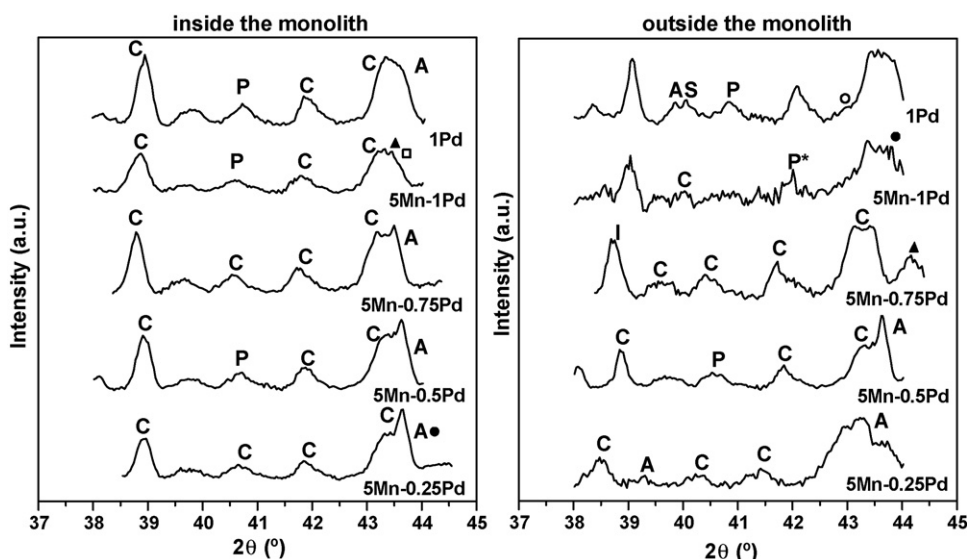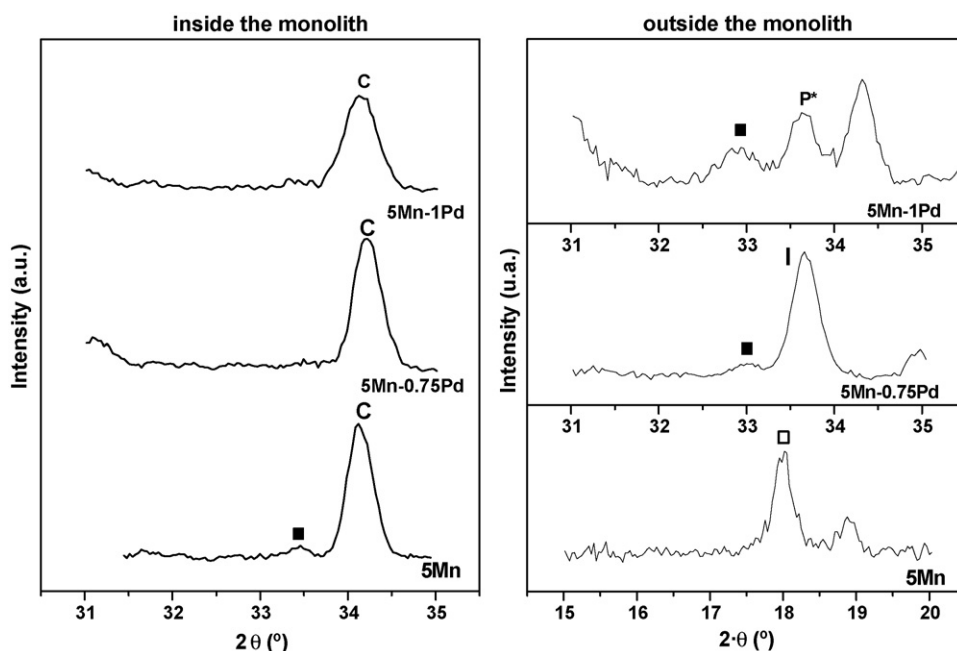

Fig. 1. Details of the X-ray diffraction patterns of samples taken after calcination (1273 K) in air (interval for the most intense diffraction peak of palladium). Where A, Al$_2$O$_3$; C, cordierite; P, Pd; P*, PdO; ●, MgAl$_2$O$_4$; ▲, MnAl$_2$O$_4$; □, Mn$_3$O$_4$; ■, Mn$_2$O$_3$; ○, 3(MgSiO$_3$·0.33Al$_2$O$_3$); AS, Al$_2$O$_3$·2SiO$_2$·3H$_2$O; I, indizalite (magnesium aluminum silicate, Mg$_2$Al$_4$Si$_5$O$_{18}$).

Fig. 2. Details of the X-ray diffraction patterns of samples taken alter calcination (1273 K) in air (interval for most intense diffraction peak of manganese oxide). Where C, cordierite; P*, PdO; ■, Mn_2O_3; I, indialite (magnesium aluminum silicate, $Mg_2Al_4Si_5O_{18}$).

catalysts. XRD patterns for 5Mn-xPd and 1Pd do not show a clear tendency for the palladium species distribution. For the catalyst with the smallest palladium loading (5Mn-0.25Pd), no palladium diffraction lines were observed. For the 1Pd, 5Mn-0.5Pd and 5Mn-1Pd catalysts, metallic palladium diffraction lines were measured. In this last catalyst PdO diffraction lines were also found. For the catalyst 5Mn-0.75Pd the presence of $LaPdO_4$ species was also detected. This behaviour could be due to the high dispersion degree of palladium reached.

3.2. Temperature-programmed oxidation

It is essential to understand how these catalysts are affected by temperature under an oxidant atmosphere. In order to analyze their behaviour, a series of temperature-programmed oxidation experiments have been carried out. The results of these TPO experiments are shown in Fig. 3. For the 1Pd catalyst three positive peaks were observed at 1015 (c), 1065 K (d) and a very small peak at 1108 K (e) during the heating. These peaks are due to oxygen release when different forms of PdO decompose into its metallic state [2,20]. During cooling one negative peak (a) at 776 K was observed. This peak is due to Pd

re-oxidation [2,20]. In the case of the 5Mn catalyst only one small positive peak was observed at 1009 K during heating. This peak could be due to the decomposition of manganese oxide species in other less O-rich ones (i.e. Mn_3O_4 to MnO). During cooling a negative peak is observed at 1097 K, this peak is due to the re-oxidation of these manganese oxide species with a lower oxidation state.

For the 5Mn-xPd catalysts, during cooling, the reoxidation peak (b) appears at clearly higher temperature (886 K) than for the palladium monometallic catalysts. This peak increases as the palladium content increases. On the other hand, the intensity of the positive peaks placed at 1015 and 1108 K was reduced in the presence of manganese. Thus, for the catalysts 5Mn-0.25Pd and 5Mn-0.5Pd, with a higher relative Mn/Pd proportion, only a single peak was observed during the heating. This peak was situated at 1065 K and it can be attributed to PdO decomposition. This PdO is observed in all 5Mn-xPd catalysts. This reduction of Pd–PdO hysteresis in the 5Mn-xPd catalysts increases the stability range of PdO with temperature as comparted to palladium monometallic catalyst. The PdO formation at higher temperature in bimetallic catalysts during cooling is associated with palladium phases in contact with

Table 3
Crystalline phases observed in the monolith washcoat after calcination in air at 1273 K

Sample	Inside the monolith channels	Outside the monolith channels
5Mn	Cordierite, $MnAl_2O_4$, Mn_2O_3	Al_2O_3, SiO_2, MgO, Mn_3O_4
1Pd	Cordierite, Al_2O_3, Pd, $Mg(OH)_2$	Cordierite, Pd, $Al_2O_3 \cdot 2SiO_2 \cdot 3H_2O$, $(MgSiO_3 \cdot 0.33Al_2O_3)$
5Mn-0.25Pd	$3(MgSiO_3 \cdot 0.33Al_2O_3)$, $MnAl_2O_4$, Al_2O_3, $MgAl_2O_4$	Cordierite, $MnAl_2O_4$, Al_2O_3, $Mg_{0.9}Mn_{0.1}$
5Mn-0.5Pd	Cordierite, $Mg(OH)_2$, Al_2O_3, Pd	Cordierite, Al_2O_3, $MgAl_2O_4$, Pd
5Mn-0.75Pd	Cordierite, Al_2O_3, $MgSiO_3$	$Mg_2Al_4Si_5O_{18}$, $MnAl_2O_4$, La_2O_3, Mn_2O_3, $LaPdO_4$
5Mn-1Pd	Cordierite, $MnAl_2O_4$, $MgAl_2O_4$, Pd, Mn_3O_4	Cordierite, $MgAl_2O_4$, $MnAl_2O_4$, Mn_2O_3, PdO
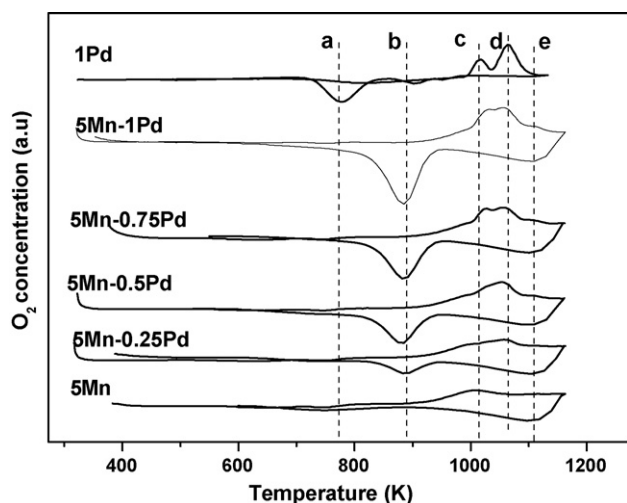
Fig. 3. TPO profiles of mono and bimetallic manganese and palladium catalysts.

Fig. 4. (a) Mn 2p XPS spectra and (b) Pd 3d XPS spectra of fresh Mn-Pd catalysts.

manganese oxides. Thus, the interaction between these two semiconductors oxides increases the oxygen mobility in the spinel phase of manganese oxide favouring the formation of palladium oxide [14,15].

3.3. Photoelectron spectroscopy (XPS)

The oxidation state and the nature of species on the monoliths surface have been analyzed by XPS. The binding energies of Al 2p, Pd $3d_{5/2}$, Mn $2p_{3/2}$ and Si 2p are summarized in Table 4. Photoelectron spectra Pd 3d and Mn 2p levels are displayed in Fig. 4a and b, respectively. All Mn $2p_{3/2}$ peak binding energies for both the monometallic (5Mn) and the bimetallic Mn-Pd fresh samples fall in a very narrow range between 641.6 and 642.0 eV (Table 4). This value is in the range reported for MnO_2 (641.7–642.2 eV) and Mn_2O_3 (641.3–641.7 eV) [21,22]. Some decrease of the binding energy for Mn $2p_{3/2}$ level with the increase in palladium amount in bimetallic system was also observed. According to this, manganese seems to be as MnO_2 in the 5Mn catalyst and for the Mn-Pd bimetallic systems it seems to be as species with lower oxygen content such as Mn_2O_3. For the palladium monometallic, the 5Mn-0.25Pd and the 5Mn-0.75Pd catalysts only one component was found at 337.1 eV. This peak corresponds to Pd^{2+}, but it is not pure PdO (336.1 eV) or Pd^{4+} (337.5 eV). The obtained value can be attributed to the interaction of PdO with alumina and/or with MnO_x phases. It cannot be excluded the contribution of both Mn and Pd oxide semiconductors interaction which shifts
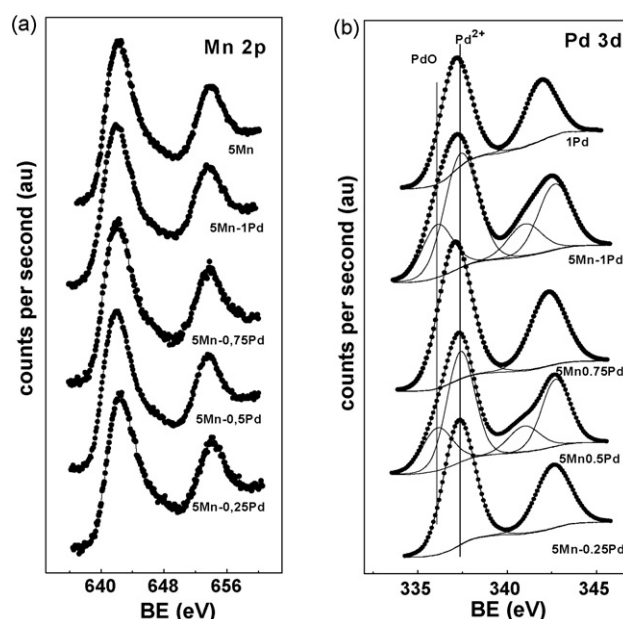
the Pd peak toward higher binding energy. For the 5Mn-0.5Pd and the 5Mn-1Pd catalysts a second component at 336.1 eV was measured. It is smaller that the other component detected and contributes with 20.3% and with 17.5% of the total Pd signals measured for these two catalysts, respectively. This peak situated at 336.1 eV may be associated with PdO.

Table 5 summarizes the surface composition derived from XPS analysis. In this table it can be observed that the catalyst with the maximum palladium surface exposure is the 5Mn-0.5Pd catalyst, but the rest Pd-Mn catalysts showed similar Pd surface exposures. Only the bimetallic catalyst with the lowest palladium content (5Mn-0.25Pd) presented a surface Pd exposure lower than the one exhibited by the Pd monometallic catalyst.

3.4. Catalysts activity

3.4.1. Lab-scale test

3.4.1.1. Effect of lambda. The activity results obtained for the 5Mn-0.5Pd catalyst at different lambda between 3 and 9 operating at 5 bar of pressure are shown in Fig. 5. Although the usual lambda in real applications uses near 3, this type of analysis was performed in order to understand the behaviour of these catalytic systems. As it can be observed in Fig. 5, only for

Table 4
Binding energies (eV) of catalysts core-levels

Catalysts	Al 2p	Mn $2p_{3/2}$	Pd $3d_{5/2}$	Si 2p
5Mn	74.5	642.0	–	102.8
1Pd	74.5	–	337.1	103.0
5Mn-0.25Pd	74.5	641.9	337.1	102.8
5Mn-0.5Pd	74.5	641.7	336.1 (21.3); 337.2 (79.7)	102.9
5Mn-0.75Pd	74.5	641.7	337.0	102.8
5Mn-1Pd	74.5	641.6	336.1 (17.5); 337.2 (82.5)	103.0

Table 5
XPS surface atomic ratios

Catalyst	Mn/Al	Pd/Al	Al/Si
5Mn	0.488	–	3.63
1Pd	–	0.011	0.41
5Mn-0.25Pd	0.317	0.005	4.13
5Mn-0.5Pd	0.332	0.025	3.07
5Mn-0.75Pd	0.238	0.021	4.44
5Mn-1Pd	0.429	0.024	3.11
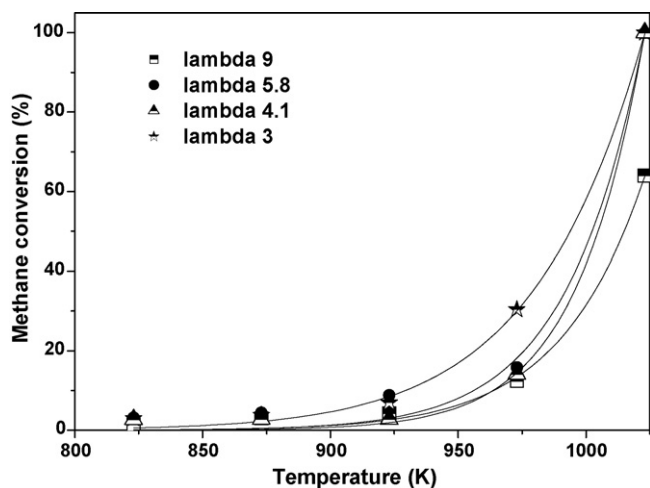
Fig. 5. Activity tests at different lambdas for 5Mn-0.5Pd monolithic catalyst.

Fig. 7. Light-off curves for mono and bimetallic manganese and palladium catalysts in methane combustion at lambda 3.

lambda 9 methane total conversion was not reached (64% of methane conversion at 1023 K). In this figure it can be also observed that the highest methane conversion at 973 K is obtained for lambda 3. At temperatures higher than 950 K the activity of this catalyst drastically increased.

For the other manganese-palladium bimetallic and manganese monometallic monolithic catalyst systems similar behaviours were observed. The palladium monometallic catalyst was more active than the Mn-containing catalysts at low temperature and showed a dip in conversion at around 923 K during the heating. This phenomenon is presented in Fig. 6 for different values of lambda. In this figure it can also be observed that for lambda 3 this phenomenon occurs at a lower temperature, around 873 K. Such a dip may be due to the effect of PdO decomposition into metallic palladium [2]. On the other hand, for this Pd catalyst high activity was observed up to 823 K, and for lambda 3 the conversion of methane was complete at 923 K.

The activity tests of the different 5Mn-xPd monolithic catalyst systems and the monometallic (Pd and Mn) monolithic catalysts at lambda 3, 5 bar of pressure and 923 K of
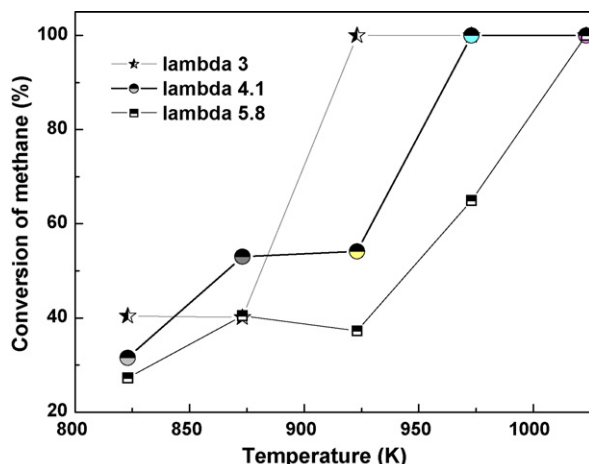

Fig. 6. Activity tests at different lambdas of the 5Mn-0.5Pd monolithic catalyst.
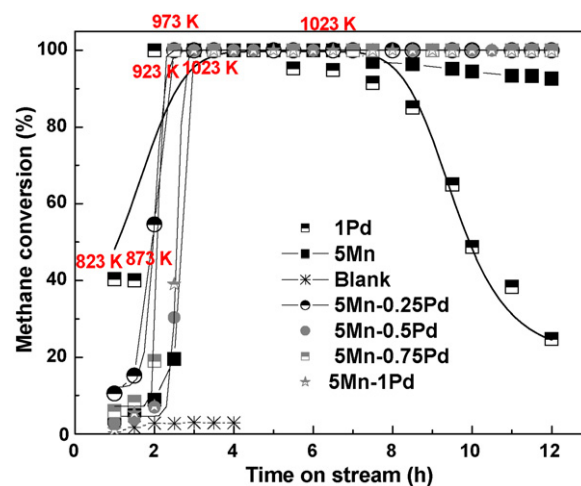
temperature are shown in Fig. 7. It this figure, the effect of the stainless steel reactor in the methane conversion is also presented (blank test). The effect of the reactor material was negligible; the conversion without catalyst was around 2.9% at 1023 K. In the same figure a slightly deactivation of the manganese monometallic catalyst can be seen. For this catalyst the methane conversion was around 92.6% after 12 h on-stream, and it is expected that the deactivation will further increase for higher times of reaction. The deactivation effect for the palladium monometallic catalyst was very important. It started being the most active catalysts, but its methane conversion decreased rapidly with the time-on-stream. The methane conversion after 12 h on-stream was around 25% for this monometallic catalyst.

The Mn-Pd bimetallic catalysts showed a stable activity. For them the only differences detected correspond to the initial stabilization period ($<$2 h). Therefore, it seems that these bimetallic 5Mn-xPd catalysts are appropriate candidates for methane combustion at high temperature because of their thermal stability. This is not the case for the palladium monometallic system. A deactivation process took place for this catalyst after 8 h on-stream. The Mn monometallic catalyst also showed some deactivation but not so important as the one showed by the Pd monometallic catalyst.

To prove the stability of these 5Mn-xPd catalysts a last experiment was performed in the lab-scale reactor. The configuration of this experiment was the following: the palladium monometallic monolith (1Pd) was used as igniter and as thermally resistant catalysts the 5Mn-0.25Pd catalyst was tested. The lowest palladium containing bimetallic system was chosen due to economic reasons. This experiment was developed at lambda 3, pressure of 5 bar and with an inlet temperature of 923 K. As it can be seen in Fig. 8, along 100 h of reaction no deactivation was observed, and total methane conversion was obtained even after 100 h on-stream.

Finally, combustion product was a mixture of CO_2 and H_2O (in all of experiments). No CO was detected in the exit gas and no NO_x were detected by the GC. NO_x emissions less than 1 ppm can be expected under the operating conditions used [4].
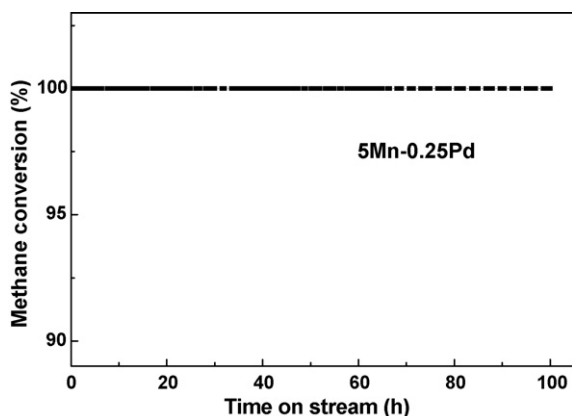
Fig. 8. Long-time activity test for the 1Pd-5Mn-0.25Pd catalyst at lambda 3 (5 bar and 923 K).

Fig. 10. Experimental data of temperature increase for Pd- and MnPd-mono-lithic catalysts in methane combustion.

3.4.1.2. Effect of the pressure. Since a gas turbine operates at pressures up to 30 bar, it is desirable to investigate the pressure impact on the catalytic activity. The experiment was designed to maintain the same linear velocity (modifying the feed flow) when the pressure was increased from 5 to 12 bar. The results obtained at the highest pressure (12 bar) with those obtained at 5 bar at the same lambda and temperature were compared and they are displayed in Fig. 9. For this comparison the 5Mn-0.5Pd catalyst was selected. A small activity decrease was observed when the pressure was increased from 5 to 12 bar. A similar total pressure effect over the methane conversion was found for the other bimetallic catalysts.

3.4.2. Pilot-plant tests

In order to confirm the activity results obtained at lab-scale for the Pd monometallic and for the Pd-Mn bimetallic monolith catalysts, new experiments were developed in a pilot plant. The catalytic combustor used contains different segments where catalysts with different properties can be arranged. In the first segment, a highly active catalyst (Pd5 with 5 wt% Pd) was used to produce the ignition at relatively low temperature. The second segment was filled with two different catalysts
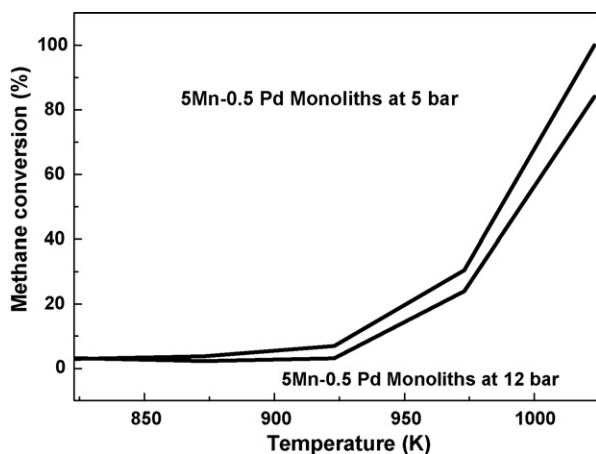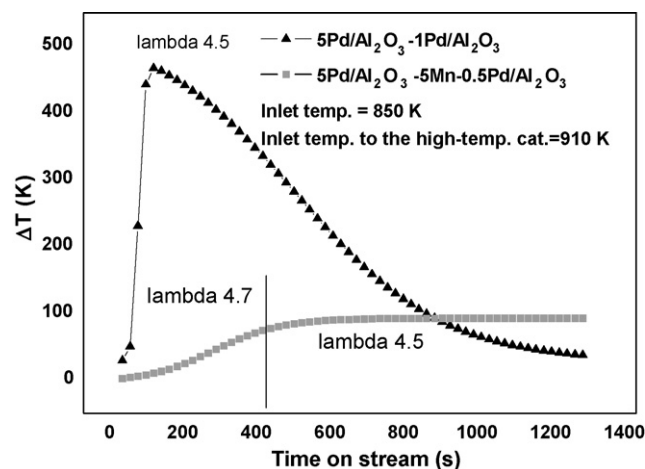
depending on the experiment being performed: Mn5-Pd0.5 or Pd1. In this pilot plant the maximum inlet temperature is over 850 K, therefore to test the Pd-Mn catalysts it was necessary to increase the temperature using igniter catalysts. The use of highly active catalysts (5Pd-1Pd) at low lambda values (lambda 3) implied that the temperature increased highly in the combustor and it was very difficult the temperature control and to prevent the flame formation. Therefore, it was decided to operate at higher lambda values (4.5–4.7) to improve the temperature control. In the two experiments the temperature was increased initially from 850 over 910 K at lambda 4.5 by the ignition catalysts. The experimental results are displayed in Fig. 10 where the temperature increase generated by the combustion reactions (the difference between the inlet temperature and the outlet temperature for the ignition and high temperature catalytic sections) is presented along the time-on-stream. As it can be observed, the catalyst behaviours were very different. In the 5Pd-1Pd test, the activity started being quiet high (big conversion). However, as the time-on-stream increased a strong decrease in activity was observed. The ignition catalyst (5Pd/Al$_2$O$_3$) operated at comparatively low temperatures and at these temperatures this catalyst is quiet stable as it was proved in the lab-scale experiments for monometallic similar catalysts (see Fig. 7). So the deactivation measured can be assigned to the high temperature catalyst (1Pd/Al$_2$O$_3$). For the 5Pd-5Mn-0.5Pd test the activity reached its steady-state after the initial activation required after each experimental lambda modification. After 800 s on-stream the activity measured using the 5Pd-5Mn-0.5Pd catalyst combination was higher than for the 5Pd-1Pd catalyst combination. These results provide additional evidence that Mn addition to Pd catalysts increases the catalytic stability when these catalytic systems are used for methane combustion.

4. Discussion

The activity test results indicate that the monometallic alumina-supported palladium monolith shows higher initial activities for methane combustion than the bimetallic 5Mn-xPd

Fig. 9. Effect of pressure in catalytic methane combustion.

catalysts. However, in both the lab-scale and in the pilot-plant reactors, the palladium monolith showed a rapid deactivation after a short time-on-stream. Nevertheless, when the bimetallic catalysts were used 12 h with total conversion of methane were achieved at the operating conditions used. A high stability for methane conversion during 100 h of reaction was measured even for the 5Mn-0.25Pd catalyst (with the lowest Pd-loading). The same behaviour is observed in the pilot-plant reactor; although the conversion was lower than in the lab-scale. This lower conversion is due to a different inlet temperature (910 K). The lab-scale experiments indicate that at higher temperatures (1023 K) the methane conversion was complete and not deactivation was observed for the 5Mn-0.5Pd/γ-Al$_2$O$_3$ catalyst. Hence, a total and stable conversion will be measured in the pilot plant if a higher inlet temperature (1023 K) in the high temperature catalytic section had been possible. In any case, the presence of Mn in the 5Mn-xPd monolithic system was able to stabilize these catalysts.

For monometallic palladium monolith when the initial increasing activities were measured when temperature was also going up, but when the temperature was kept constant at 1023 K a quick deactivation process was observed. This is in agreement with results from other authors [14,23–25]. This phenomenon of deactivation is a consequence of the decomposition at the reaction temperature of 1023 K (TPO) of PdO into metallic Pd, which is less active than the PdO [2]. The presence of PdO was confirmed by the good correlation between TPO and XPS results. The absence of PdO diffraction lines could be due to the extremely high cordierite content that could be masking this PdO phase, as well as to the small palladium oxide particle size, that could layout the detection limit of this technique (4 nm).

The high deactivation rate (methane conversion decreased from 100 to 24.5% after 7 h on stream) found for the palladium monometallic system can be attributed to the strong sintering suffered by the palladium phase during the conditions imposed in the activity tests, as it was reported in a previous work [14]. In the present one a similar effect may be occurring but not so intense because this monolithic catalyst was calcined at a higher temperature. Other deactivation problem such as palladium evaporation were not observed in this work [14], therefore at reaction temperatures up to 1273 K no significant palladium evaporation is expected. These results are in good agreement with the results reported by several authors [8–10] for experiments performed at temperatures up to 1273 K.

As shown in this previous work [14], the incorporation of manganese into the palladium catalysts prevents the deactivation. In all bimetallic 5Mn-xPd catalysts the presence of PdO (XPS, TPO) was confirmed, nevertheless only in the 5Mn-1Pd was possible to observe it by XRD. In the TPO analysis, the 5Mn-xPd catalysts showed clearly that manganese affects the PdO decomposition. It is known that the spinel phase of manganese oxide and also, Mn$_2$O$_3$, can adsorb oxygen and act in an oxidizing atmosphere like p-type semiconductors [26]. By the other hand, it has been reported in literature that the introduction of additives consisting on noble metals such as Pd, to a semiconductor metal oxide [27], modifies the microstructure and properties of metal oxide. This change in the TPO

profiles due to the Mn presence can be attributed to an increase in the oxygen mobility in the spinel phase of manganese oxide which is associated with palladium phases in contact with manganese oxides [28]. Palladium appears to weaken the Mn–O bond, thus increasing the mobility of the lattice oxygen. This active oxygen reoxidizes Pd clusters which were reduced to PdO during the oxidation of hydrocarbon [25]. And this effect of reoxidation is very clear in the 5Mn-xPd catalysts TPO results. The higher active oxygen availability from the 5Mn-xPd interface in bimetallic systems produces less metallic Pd formation, therefore this system could maintain methane total conversion during all the time of the experiment presented in this work. In addition, the Mn addition to the Pd catalysts improves the palladium dispersion at the surface of the catalysts (XPS) and this is another important factor to be considered in order to explain the more stable behaviour of Mn-Pd monoliths. Furthermore, it seems that the formation of species as MnAl$_2$O$_4$ (XRD) improves the thermal stability of the catalysts, allowing higher reaction temperatures using palladium based catalysts [6].

Finally, the Mn monometallic catalyst deactivation must be the result of, at least, two different processes. In a previous work [14], it was discussed that this deactivation can be assigned to active phase sintering and coke formation and it is possible that the same deactivation detected in this experimental work is due to the same causes.

Other interesting measured effect deal with influence of lambda on methane combustion. This influence is very similar for all the catalysts investigated. When the lambda decreases (more methane in the feed) the methane conversion increases. This is due to higher combustion temperature for the same inlet temperature because of more heat being produced when higher methane amounts are being burned. Another important result is the total pressure effect on methane conversion. For all the catalysts higher combustion pressures were associated with lower methane conversions. Chou et al. [29] investigated numerically this pressure effect and found that two opposite factors affect the overall methane conversion when pressure is changed. First, the reactant diffusion rates through the gas to the catalyst surface decrease with increasing pressure because of the negative effect of pressure on the diffusivities. Second, surface reaction rates increase with pressure due to a higher surface temperature associated to bigger heat release from the combustion reaction. Evaluation of these two factors proved that a decrease in methane conversion with pressure must be expected because the combustion is largely controlled by gaseous fuel diffusion rate at high pressures. This effect explains the small methane conversion decrease measured when pressure was increased from 5 to 12 bar (Fig. 9).

5. Conclusions

The reported results show that monometallic palladium catalysts supported on alumina present a high activity but a poor stability. The same tendency was observed for monometallic manganese monolith catalysts, although it presents not so high initial activity and a lower deactivation rate. However,

large differences in catalyst stability were found between mono- and bimetallic systems. Thus, 5Mn-*x*Pd bimetallic catalysts showed far better stability as it is proved for the 5Mn-0.25Pd catalyst being able to maintain total methane conversion along a 100 h activity test, and the same tendency was observed in the pilot-plant reactor experiments. This stability can be explained as the result of significant PdO amounts not reduced to metallic Pd because of increased oxygen mobility in the spinel phase of the manganese oxide. As a result the 5Mn-*x*Pd monolith systems seems to be promising candidates for natural gas combustion thermally resistant catalysts.

Acknowledgements

References

[1] W.C. Pfefferle, J. Energy 2 (1978) 142.
[2] K. Persson, A. Ersson, K. Jansson, J.L.G. Fierro, S.G. Järas, J. Catal. 243 (2006) 14.
[3] Y. Ozawa, Y. Tochichara, N. Mori, I. Yury, J. Sato, K. Kagawa, Catal. Today 83 (2003) 247.
[4] R.A. Dalla Betta, Catal. Today 35 (1997) 129.
[5] D. Ciuparu, M.R. Lyubovsky, E. Altman, L.D. Pfefferle, A. Datye, Catal. Rev.-Sci. Eng. 44 (2002) 593.
[6] S.A. Yashnik, Z.R. Ismagilov, V.V. Kuznetsov, V.V. Ushakov, V.A. Ovsyannikova, Catal. Today 117 (2006) 525.
[7] P. Euzen, J.-H. Le Gal, B. Rebours, G. Martin, Catal. Today 47 (1999) 19.
[8] J.J. Spivey, J.B. Butt, Catal. Today (1992) 465.
[9] L.L. Hegedus, J.C. Summers, J.C. Schlatter, K. Baron, J. Catal. 56 (1979) 321.
[10] J.G. McCarty, M. Gusman, D.M. Lowe, D.L. Hildenbrand, K.N. Lau, Catal. Today 47 (1999) 5.
[11] Y. Ozawa, Y. Tochihara, A. Watanabe, M. Nagai, S. Omi, Appl. Catal. A: Gen. 258 (2004) 261.
[12] K. Narui, H. Yata, K. Furuta, A. Nishida, Y. Kohtoku, T. Matsuzaki, Appl. Catal. A: Gen. 179 (1999) 165.
[13] H. Arai, M. Machida, Catal. Today 10 (1991) 81.
[14] V.A. de la Peña O'Shea, M.C. Alvarez-Galvan, J. Requies, V.L. Barrio, P.L. Arias, J.F. Cambra, M.B. Güemez, J.L.G. Fierro, Catal. Commun. 8 (2007) 1287.
[15] Y. Tsuji, S. Imamura, in: T. Inri, et al. (Eds.), New Aspects of Spillover Effect in Catalysis, Elsevier, Amsterdam, 1993, p. 405.
[16] T. Ishihara, H. Shigematsu, Y. Abe, Y. Tanaka, Chem. Lett. (1993) 407.
[17] R.A. Della Betta, K. Tsurumi, T. Shoji, R.L. Garten, US Patent 5405, 260 (1995).
[18] A.F. Ahlström-Silversand, C.U.I. Odenbrand, Appl. Catal. A: Gen. 153 (1997) 157.
[19] J.C.G. Andrae, D. Johansson, M. Bursell, R. Fakhari, J. Jayasuriya, A. Manrique-Carrera, Appl. Catal. A: Gen. 293 (2005) 129.
[20] G. Groppi, C. Cristiani, L. Lietti, P. Forzatti, in: A. Corma, F.V. Melo, S. Mendioroz, J.L.G. Fierro (Eds.), Stud. Surf. Sci. Catal., vol. 130, Elsevier, Amsterdam, 2000, p. 3801.
[21] L.S. Cheng, R.T. Yang, N. Chen, J. Catal. 164 (1996) 70.
[22] P. Papaethimiou, T. Ioannides, X.E. Verykios, Appl. Catal. B: Env. T15T (1998) 75.
[23] S. Colussi, C. de Leitenburg, G. Dolcetti, A. Trovarelli, J. Alloys Compd. 374 (2004) 387.
[24] H. Yamamoto, H. Uchida, Catal. Today 45 (1998) 147.
[25] V.A. de la Peña, M.C. Alvarez-Galvan, J.L.G. Fierro, P.L. Arias, Appl. Catal. B: Env. 57 (2005) 191.
[26] M. Baldi, V.S. Escribano, J.M.G. Amores, F. Milella, G. Busca, Appl. Catal. B: Env. 17 (1998) 175.
[27] A. Cabot, A. Diéguez, A. Romano-Rodríguez, J.R. Morante, N. Bârsan, Sens. Actuators B 79 (2001) 98.
[28] H.F.J. van't Blik, R. Prins, J. Catal. 97 (1986) 188.
[29] C.P. Chou, J.Y. Chen, G.H. Evans, W.S. Winter, Combust. Sci. Technol. 150 (2000) 27.